Supporting Information

Enhanced therapeutic potential of AEBP1 silencing via engineered apoptotic mesenchymal stem cell-derived nanovesicles in atrial fibrillation

Gyeongseo Yoo[1], Ji-Young Kang[2], Malgeum Park[2], Jaewoong Lee[2], Dasom Mun[2], Nuri Yun[3*], Boyoung Joung[1,2*]*

[1]Graduate School of Medical Science, Brain Korea 21 Project; [2]Division of Cardiology, Yonsei University College of Medicine, Seoul, 03722, Republic of Korea, Yonsei University College of Medicine, Seoul, 03722, Republic of Korea; [3]GNTPharma Science and Technology Center for Health, Incheon, 21983, Republic of Korea

*Correspondence: Boyoung Joung, Division of Cardiology, Yonsei University College of Medicine, Seoul, 03722, Republic of Korea, Email cby6908@yuhs.ac; Nuri Yun, GNTPharma Science and Technology Center for Health, Incheon, 21983, Republic of Korea, Email yunnuri@hanmail.net; Dasom Mun, Division of Cardiology, Yonsei University College of Medicine, Seoul, 03722, Republic of Korea, Email christsom@yuhs.ac

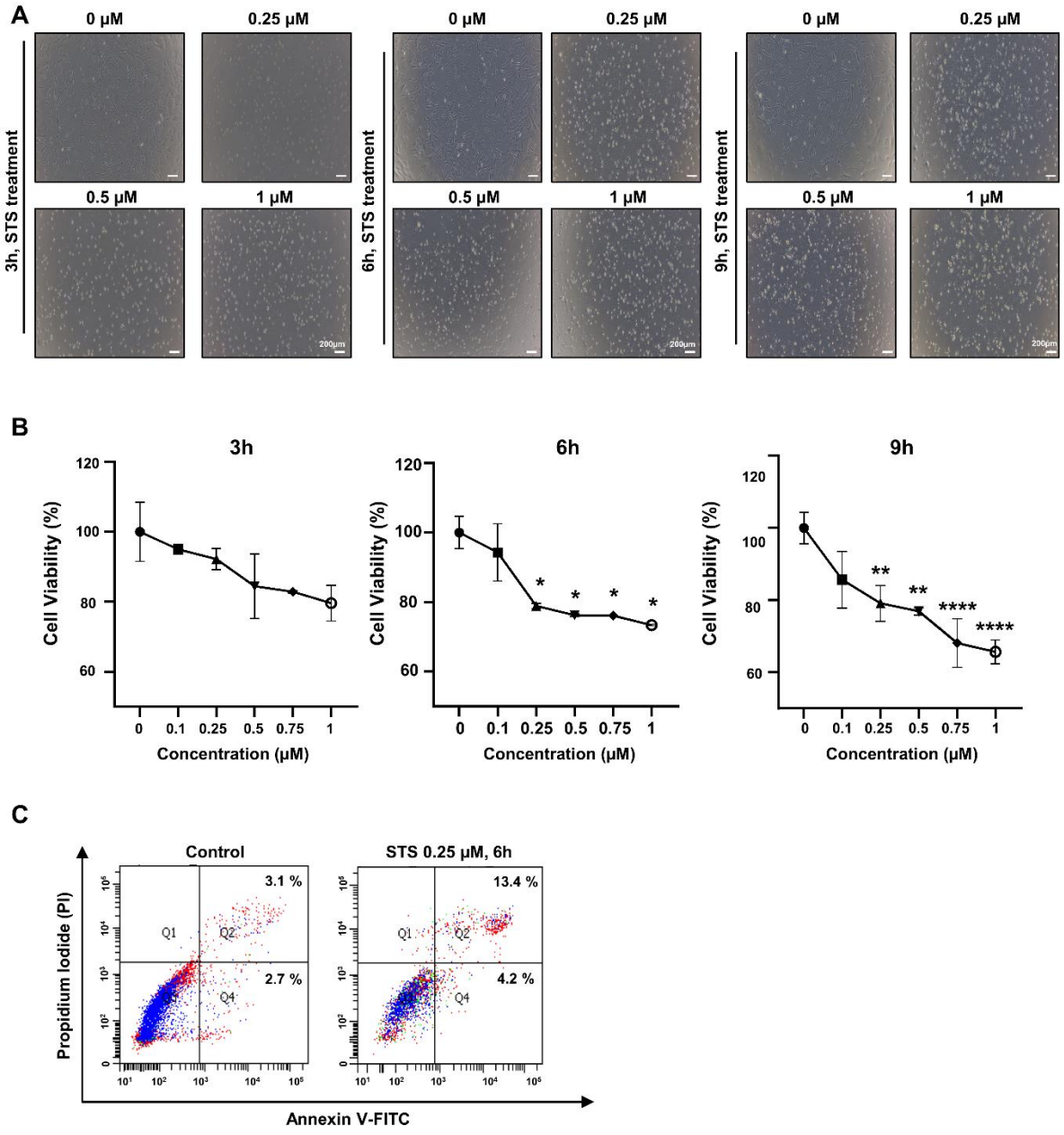

Figure S1. Staurosporine (STS) treatment of MSCs. A) Time- and dose-dependent morphological changes in MSCs following STS treatment. Scale bar = 200 µm. B) Cell viability assay of MSCs exposed to STS over varying durations and concentrations. C) Representative flow cytometry plots using Annexin V-FITC/PI staining for apoptosis; FITC, fluorescein isothiocyanate; PI, propidium iodide. *$P < 0.05$, **$P < 0.01$, ****$P < 0.0001$

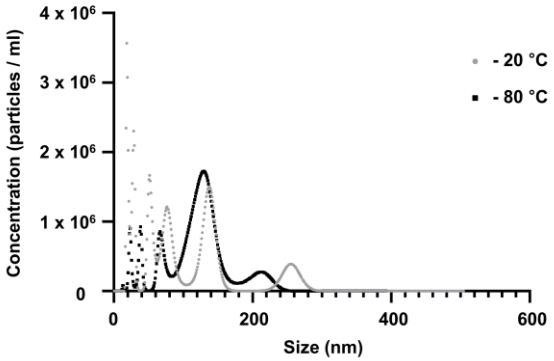

Figure S2. Particle size and concentration of ANVP after storage at -20 °C and -80 °C.

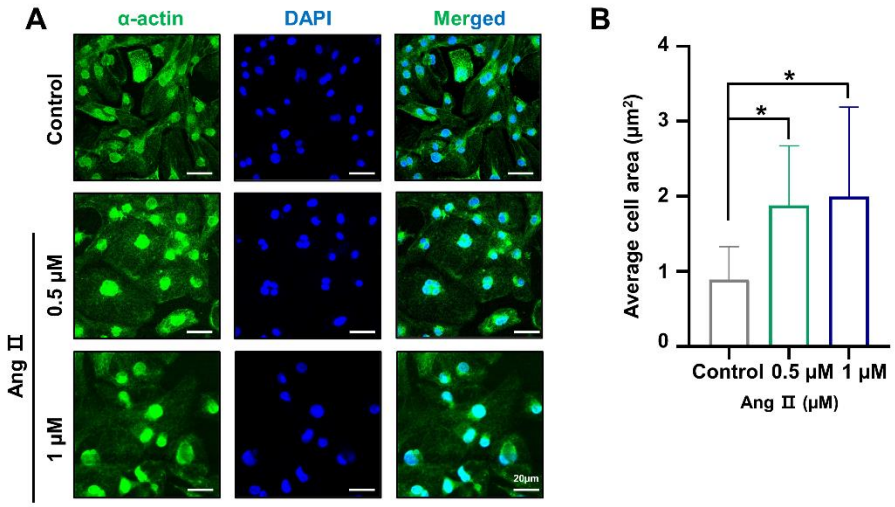

Figure S3. Dose optimization of Ang II for inducing AF-like phenotype in iPSC-aCMs *in vitro*. A, B) Representative immunofluorescence images and quantitative analysis showing enlargement of cell surface area via α-actin staining (green). Nuclei were counterstained with DAPI (blue). Scale bar = 20 μm. *$P < 0.05$

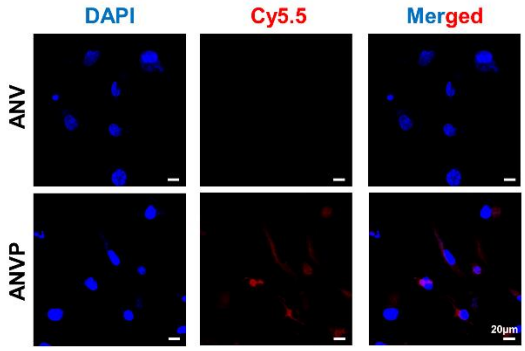

Figure S4. Evaluation of Cy5.5-labelled ANVP (red) binding affinity to iPSC-aCMs cell surface. Nuclei were counterstained with DAPI (blue). Scale bar = 20 μm.

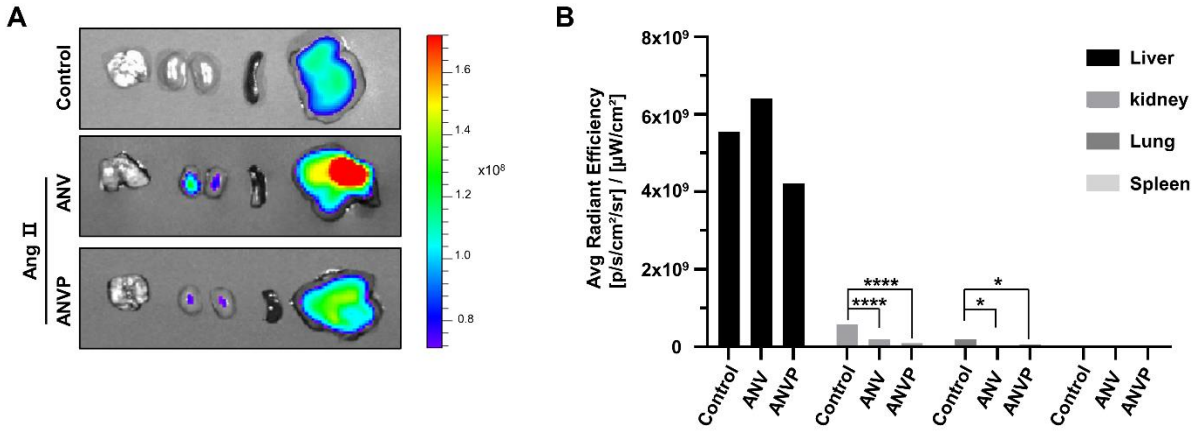

Figure S5. *In vivo* biodistirbution of ANVP. A, B) Representative IVIS images and quantified data showing fluorescence intensity in different organs of mice at 4h after intravenous injection of PBS in untreated mice, ANV, and ANVP in Ang Ⅱ-treated mice (n = 3 per group). *$P < 0.05$, ****$P < 0.0001$.

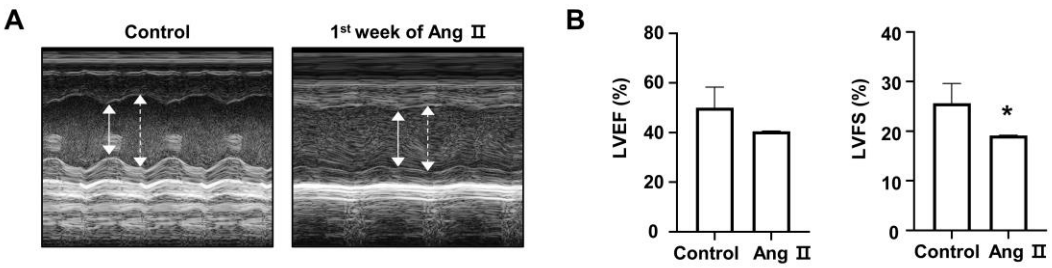

Figure S6. Echocardiographic assessment of cardiac function one week after Ang II pump implantation: representative M-mode images and quantification of EF and FS (n = 3 per group). *$P < 0.05$

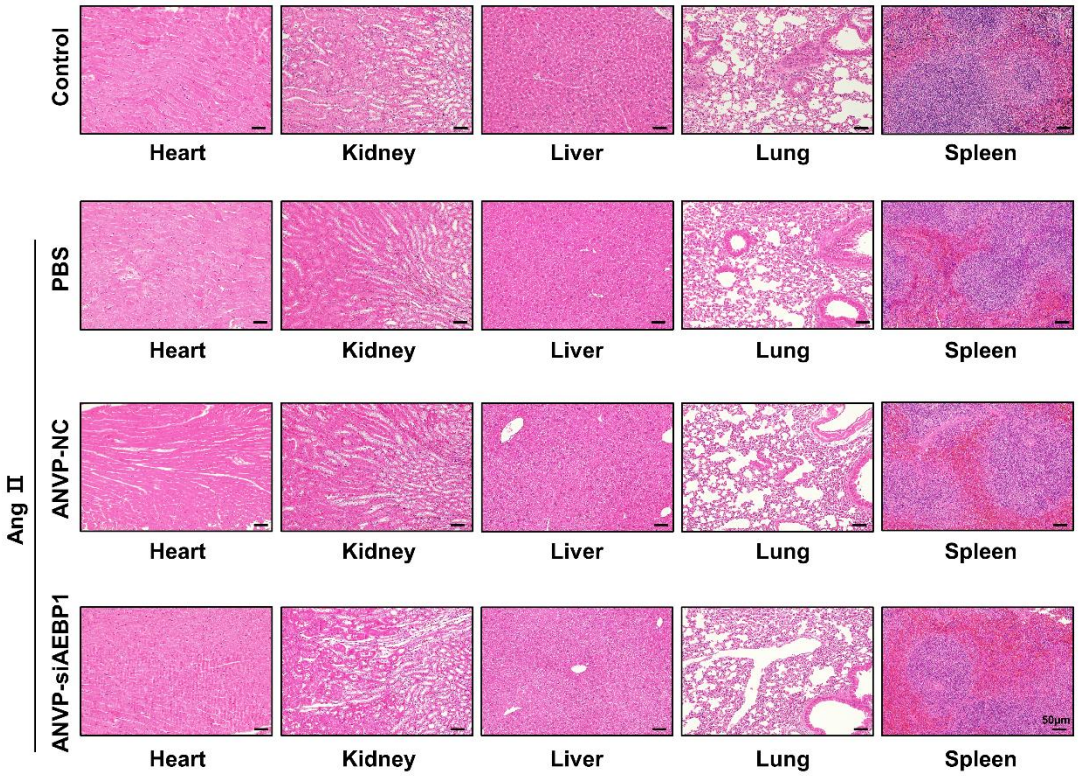

Figure S7. Representative images of H&E-stained different organs (Heart, Kineys, Liver, Lung, and Spleen) after intragenous injection of PBS, ANVP-NC, ANVP-siAEBP1, Scale bar = 50 μm.

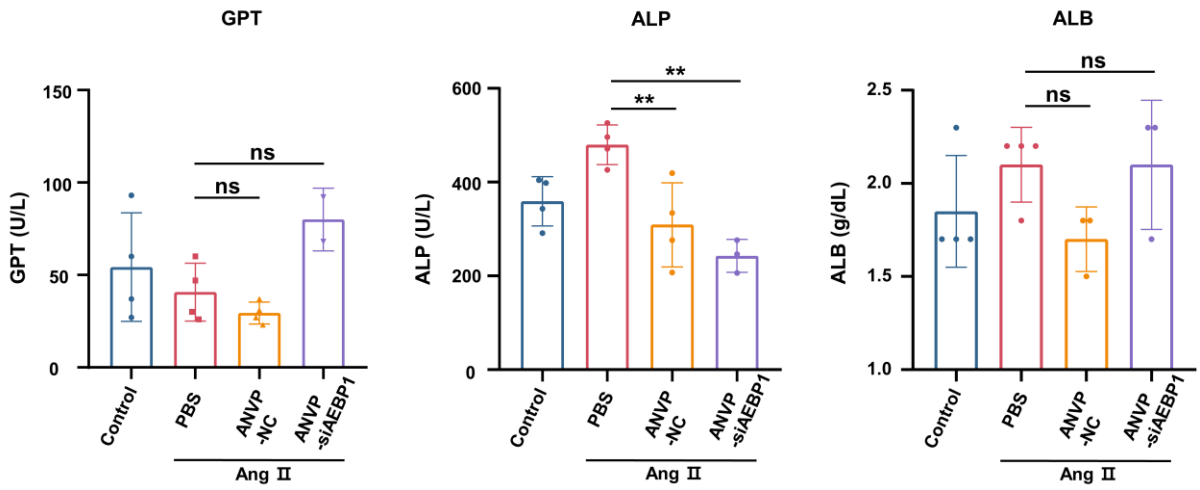

Figure S8. Levels of GPT, ALP, and ALB in serum of mice after intravenous injection of each samples. $^{**}P < 0.01$.

Table S1. The clinical profiles of study subjects

Variables	**Non-HF (*n* = 5)**	**HF (*n* = 5)**	***P* value**
Age, years	65.0 (63.5-68.0)	64.0 (63.0-72.5)	0.916
Male, n (%)	2 (40)	4 (80)	0.197
BSA (m^2)	1.53 (1.53-1.87)	1.71 (1.47-1.89)	0.751
Hypertension, n (%)	3 (60)	3 (60)	1.000
Diabetes mellitus, n (%)	0 (0)	3 (60)	0.038
Stroke, n (%)	0 (0)	0 (0)	N/A
LAD, mm	40.0 (33.0-41.5)	49.0 (43.5-51.5)	0.009
LVEF, %	66.0 (46.5-74.0)	37.0 (24.5-50.5)	0.076

Values are expressed as n (%) or median (interquartile range).

BMI, body mass index; LAD, left atrial diameter; LVEF, left ventricular ejection fraction.

Table S2. List of primers used for qRT-PCR (Human)

Gene	Forward (5'-3')	Reverse (5'-3')
MLC3	CAAGGACACAGGCACCTATGAG	CTCCACTTCGTCTTCTGTCAGC
AEBP1	CTATGACATCGGGGCCACTC	CCTTCCATGTGCTGATGGGT
GAPDH	GGAGCGAGATCCCTCCAAAAT	GGCTGTTGTCATACTTCTCATGG

Table S3. List of primers used for qRT-PCR (Mus musculus)

Gene	Forward (5'-3')	Reverse (5'-3')
MLC3	TGCCTCCAAGATTAAGATCGAGT	CTCTGCCTGGGTAGGATTCTG
AEBP1	GAGGTGGTAACTACTGACAGCC	CCAGGCTGTATGTGCGAGTGAT
IL-1β	TGGACCTTCCAGGATGAGGACA	GTTCATCTCGGAGCCTGTAGTG
TNF-α	GGTGCCTATGTCTCAGCCTCTT	GCCATAGAACTGATGAGAGGGAG
iNOS	ACATCGACCCGTCCACAGTAT	CAGAGGGGTAGGCTTGTCTC
Collagen I	AAGGGTCCCTCTGGAGAACC	TCTAGAGCCAGGGAGACCCA
COL3a2	TCAAGTCTGGAGTGGGAGG	TCCAGGATGTCCAGAAGAACCA
α-SMA	GCATCCACGAAACCACCTA	CACGAGTAACAAATCAAAGC
GAPDH	CATCACTGCCACCCAGAAGACTG	ATGCCAGTGAGCTTCCCGTTCAG